Drone RCS Statistical Behaviour

Pavel Sedivy/ Ondrej Nemec
RETIA, a. s.
Pardubice
CZECH REPUBLIC

E-mail: psedivy@retia.cz / onemec@retia.cz

ABSTRACT

The drones are becoming widespread continuously. Risks of drones misuse poses challenges for its radar detection. The paper presents the results of the measurement and analysis of several nano and micro size UAVs (drones) Radar Cross Section (RCS). Presented results were measured in far-field in X-band. Measured drones include quad-copters, hexacopters and fixed-wing 2 m wingspan glider. Subsequent measurement results analysis focuses on the RCS statistical properties. The results can be utilised for automated target recognition and detection performance evaluation. No restrictions for presentation nor publication of paper in meeting proceeding applies, the paper is not subject of classification and is intended for public release.

1.0 INTRODUCTION

The monostatic primary radar signature of drones is often characterised by Radar Cross Section (RCS) as a single number. This is far from the truth. The radar cross-section varies with observation angles and slightly fluctuates with frequency. Paper presents the results of RCS measurement of several drones of nano and micro UAV category.

Drones RCS was measured in an anechoic chamber using the far-field setup in X-band. Measurement was performed by vector network analyser with time-domain post-processing. The measurement validity was verified by measurement of background reflection (RCS). RCS was evaluated for several frequencies over a frequency band and for several elevation angles.

Measurements were performed for several drones – multi-copters, fixed wings and some components. Results are presented in the form of RCS azimuth polar plot, statistics and cumulative density function plot.

Similar RCS measurements and modelling were already published on several conferences and papers, e.g. [1, 2]. All these papers focus on a single number or single plot representation of RCS. More detailed analysis is presented in [3] and focuses on ISAR evaluation of drones' component contribution to overall RCS. Another paper [4] analyses DJI's Phantom rotor blade RCS, if it were made of aluminium.

Although drones tilts in both pitch and roll to fly, all published RCS charts and values were measured at horizontal plane (zero pitch and roll).

The presented analysis of the real drones RCS behaviour over varying aspect angle and carrier frequency gives an opportunity for classification (non-cooperative target recognition) based on RSC time series and frequency caused fluctuation behaviour and real drone detection performance estimation. Analyses are supported by short analysis of drone flight telemetry data to include context.

Next part of the paper continues with Approach describing measurement methods and conditions, followed by chapters Results and discussion and Future work. The results are summarized in chapter Conclusion.

2.0 APPROACH

Paper presents the results of two activities, drones' RCS measurement and subsequent statistical analysis. Results are put in observation scenario context by additional analysis of copter type drone telemetry data.

2.1 RCS measurement method

Radar Cross Section was evaluated from far-field transition measurement between transmission and reception antenna performed by Vector Network Analyser (VNA). Measurement setup is illustrated on Fig. 1.

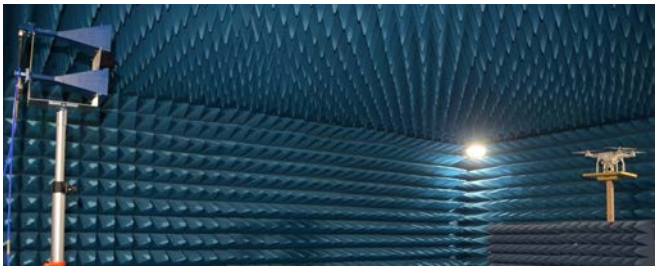

Fig. 1. Drone RCS measurement

Method of measurement was very similar to those described in [1], but as reference was used 300 mm stainless steel ball instead of metallic plate.

The Device (Drone) Under Test – DUT were rotated in horizontal plane and illuminated by reference signal – harmonic wideband sweep generated by Vector Network analyser. For every position in turn were received reflected signal by separate antenna.

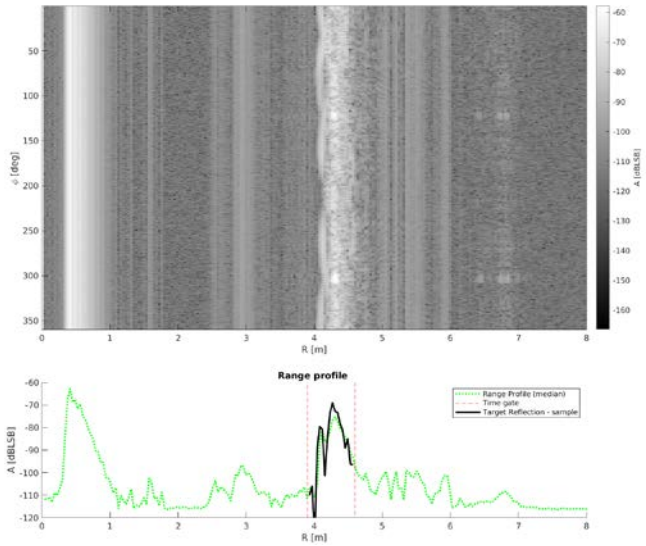

Fig. 2. Drone trajectory – mix of pre-planned mission and manual control

The received signal was evaluated, interpreted as transmission ratio s21 and stored. Stored s21 values over frequency for each direction were zero padded to avoid periodic aliasing and converted to time (range) profile by inverse DFT. An example output of this processing is depicted on Fig. 2. This picture illustrates

individual components of received signal – cross talk (at the lowest ranges) and few reflections caused by imperfection of anechoic chamber. All of them are close to constant. The only varying component is reflection caused by DUT – observed drone. The signal components outside DUT reflection is suppressed by windowing and converted back into frequency domain by direct DFT.

The antennas cross talk and reflections on other ranges (outside measured drone at distance of 4 m) was suppressed by range (time) domain windowing. This pre-processed signal is converted for each azimuth position back to frequency domain. Received signal is normalised by signal (transmission) measured for stainless steel 300 mm reference ball.

Measured RCS can be presented either for single frequency or as a statistic over selected band.

2.2 Radar observation scenario of drones

RPASs/UAVs/drones monostatic Radar Cross Section should be evaluated over complete range of parameters occurring in real observation scenario. These parameters must include variation of radar operation parameters and drone observation aspect angles over relative position to radar and drones' flight modes. Aspect angles of drone observation consist of two principal components, drone pitch/roll position and relative angular position of radar and radar.

Copter type drones utilizes set of motors to generate both lift and thrust. Half of propellers rotate clock-wise, while second half rotates counter clock-wise to mutually compensate reaction moment. Zero thrust requires balanced both left/right and front/rear motors pairs to keep frame levelled. Horizontal movement is achieved by tilting the drone in pitch/roll coordinate. This tilt converts part of lift into thrust [5,6].

Real drone flight behaviour was analysed using a Robodrone's Hornet drone autopilot (ARDUPILOT [7]) telemetry log. The analysed mission was mixture of pre-planned mission/manual flight with top speed of 10 m/s. The trajectory is depicted on Fig. 3, chart of drone roll over time and cumulative density function of drone roll are on Fig. 4.

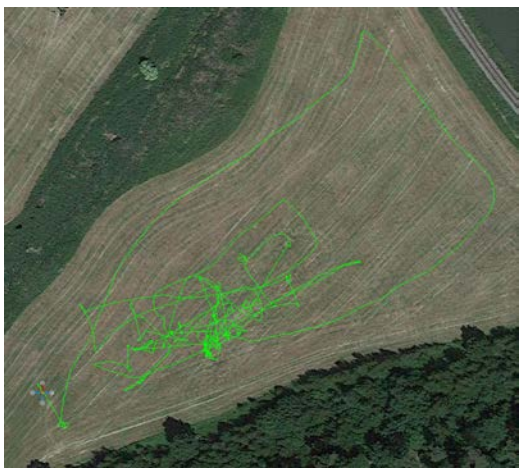

Fig. 3. Drone trajectory – mix of pre-planned mission and manual control

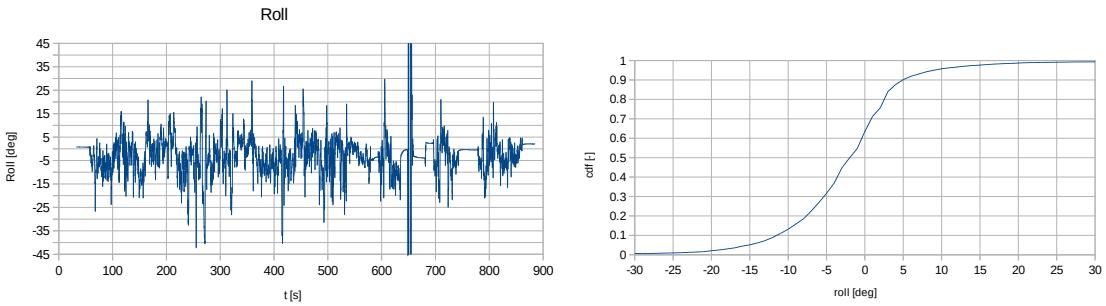

Fig. 4. Drone roll over time (left) and corresponding cumulative density function (right)

Figures shows drones' roll behaviour for single flight and disclose general rare occurrence of zero roll. For real drone's flight roll (and according to our analysed data pitch) fluctuates in range ±20 degrees.

As low flying copter type drones are observed by radar with much lower aspect angle, drone tilt caused by flight control determines observation scenario. Radar cross section should be evaluated within real extent of angular position (tilt) of drone relative to radar.

2.3 Reference to published information

Drones' RCS was measured, simulated and published in many papers over recent years. Presented results were typically measured or simulated from side views – horizontal plane and represented by single azimuth chart or even as a single value. Typical X-band RCS values for DJI Phantom family is few hundredths, about 0.02 sqm [3, 8].

2.4 RSC measurement scenarios

Drones' RCS was measured in different planes (main horizontal plane, drone nose down, drone on side) and from different elevation angles. Observation angles were changed by altering antenna height with drone in normal position on turn table.

Measurements were performed for several drones – both copter type and fixed wing. Drones was of different size within micro and small mini size categories. In addition were drones made of various materials – metallic, plastic and composites. Measurement included DJI Phantom 2, DJI Phantom 4, DJI F550, Yuneec MANTIS, Robodrone Hornet, coaxial drone Y6, coaxial drone X8, Tarot 680 Pro hex and fixed wings Pelikan GAMA 2100. In addition were measured RCS of a "payload" – outdoor camera and plastic propeller.

Turntable was mostly covered by pyramidal absorbers, the only visible part was balsa wood shaft and low density polyurethane foam table. Measured background including turn table RCS median was about 0.001 sqm.

2.5 Statistical RCS analysis

Different statistics of measured drones' RCS was evaluated to characterize behaviour – observation elevation angle, frequency. These statistics gives opportunities for improvement of radar drone detection performance estimation and target type classification.

3 RESULTS AND DISCUSSION

To provide comprehensive information on drones RCS and extend previously published on drones' monostatic radar visibility (RCS) was measured and analysed RCS from different observation angles and for different observation planes.

Measurement end evaluation of RCS was performed over wide frequency band. RCS data is presented for selected single frequency of 9 GHz and for gain available from frequency diversity observation over different frequency band.

Figure 5 presents the polar plot of the DJI Phantom 4 (diagonal size 350 mm) radar cross-section over different elevation angles. The RCS behaves quite random over azimuth and can be considered as a random variable. Estimates of cumulative density function (cdf) over different elevation angles are presented in the same figure. The cdf plot discloses consequences of the RCS randomness to detection performance estimation. Once e.g. median of the RCS is used for detection performance estimation, observed RCS will be smaller than expected in half cases. As the typical requirement for probability detection is 0.8 to 0.9, an additional 5 to 8 dB (fluctuation) losses must be considered.

Some key statistics of the Phantom's RCS is summarized in Table 1.

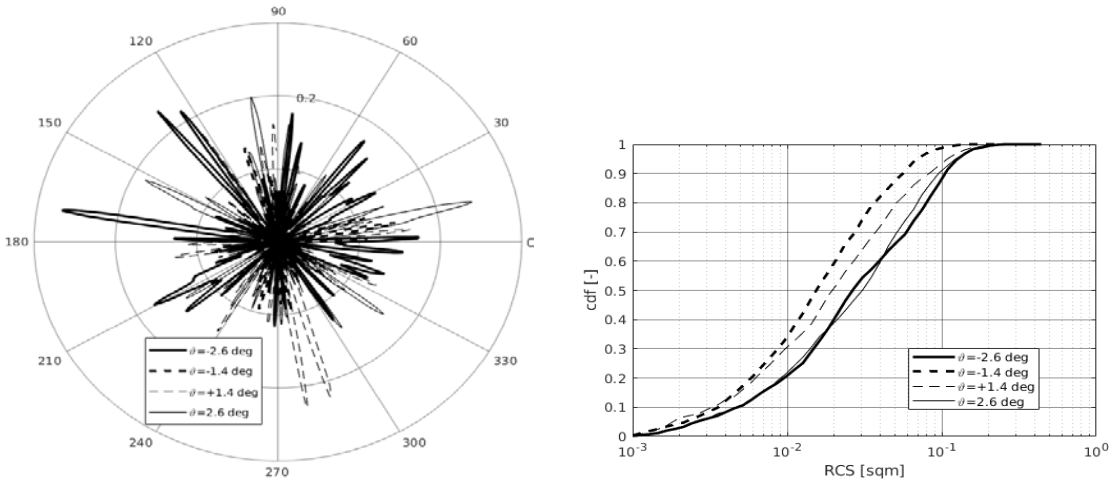

Fig. 5. Polar plot of Phantom 4 RCS [sqm] (left) and RCS cumulative density function; different elevation angles of observation, 9 GHz

Table 1. DJI Phantom 4 RCS over azimuth statistics (@9 GHz)

ϑ [°]	*RCS [sqm]*			
	max	**median**	**mean**	**10th percentile**
-2.6	0.27	0.030	0.05	0.005
-1.4	0.15	0.017	0.03	0.004
0	0.14	0.02	0.04	0.004
+1.4	0.23	0.022	0.04	0.003
+2.6	0.25	0.034	0.05	0.005

For large tilt (all roll, pitch and combined) towards/outwards the radar RCS rises.

Another observation scenario is horizontally flying multicopter drone flying in random direction relative to radar. This scenario was evaluated by measurement main horizontal plane of tilted DJI Phantom 4, see Figure 6.

Fig. 6. Measurement setup for tilted (roll 28 degrees) Phantom 4.

Measurement results are presented on Figure 7 and in Table 2. Observed RCS statistics are very close to RCS of values observed with no tilt.

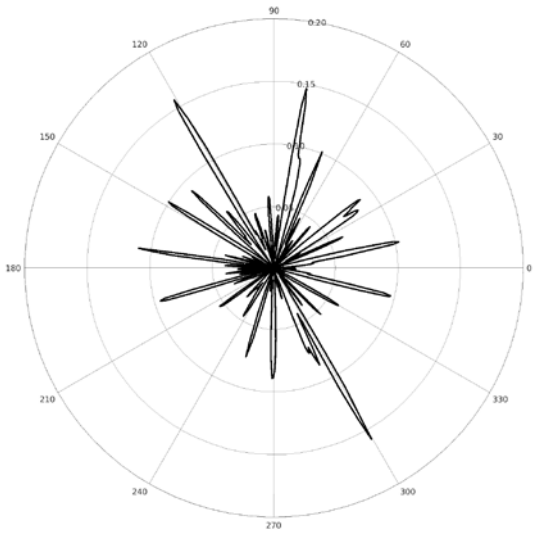

Fig. 7. Polar plot of 32 deg.pitched Phantom 4 RCS [sqm] @9 GHz.

Table 2. DJI Phantom 4 RCS over azimuth statistics (@9 GHz)

Scenario	RCS [sqm]			
	max	median	mean	10th percentile
Pitch 32 deg	0.18	0.02	0.03	0.004
Roll 28 deg	0.13	0.02	0.03	0.003

Another measurement was performed on an older DJI Phantom 2 VISION. The results are very close to results for Phantom 4. Measured RCS is presented on Figure 8. Measured maximum RCS was 0.18 sqm, median 0.02 sqm, mean 0.03 sqm and 10th percentile 0.002 sqm.

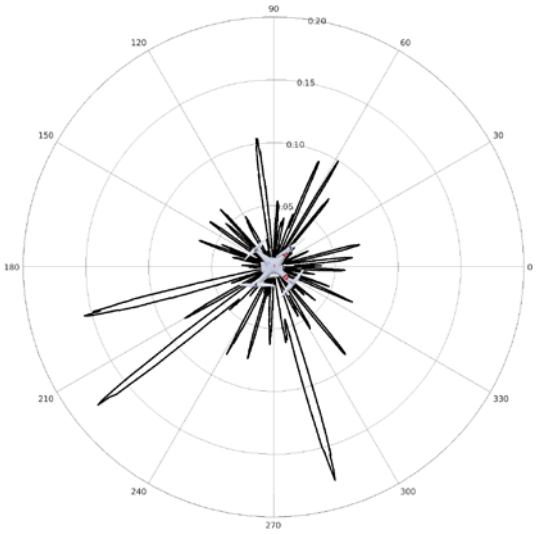

Fig. 8. Polar plot of Phantom 2 Vision RCS [sqm] @9 GHz.

Another measured quad-copter drone was Robodrone Hornet (see Figure 9). This drone consists of PLA 3D printed components assembled on carbon composite base plate.

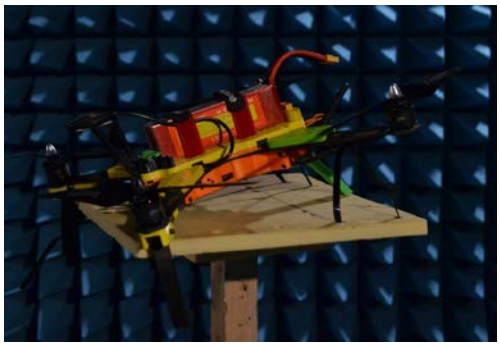

Fig. 9. Robodrone Hornet drone (16 deg nose down)

Hornet's RCS measurement results are presented in Figure 10 and in Table 3.

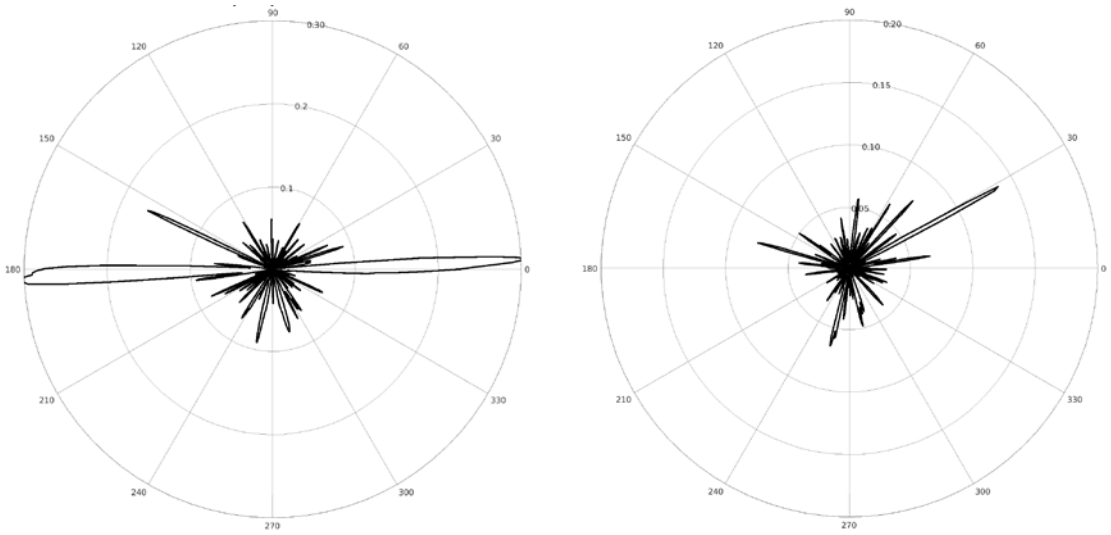

Fig. 10. Polar plot of Hornet main plane RCS (left) and 32 deg rolled UAV RCS (right); [sqm] @9 GHz.

Extreme reflection at zero and 180 degree is caused by side wall of Li-Po battery pack. Once the drone was measured rolled, waves are reflected aside of illumination direction and drones RCS significantly dropped.

Table 3. Robodrone Hornet RCS over azimuth statistics (@9 GHz)

Scenario	RCS [sqm]			
	max	median	mean	10th percentile
main	0.31	0.02	0.03	0.002
Pitch 16 deg	0.43	0.02	0.04	0.004
Pitch 25 deg	0.44	0.02	0.03	0.003
Roll 32 deg	0.15	0.01	0.02	0.003

Despite of completely different design of this drone is RCS very similar to DJI Phantom with similar dimension (Hornet diagonal size is 440 mm).

The smallest measured quad-copter drone was Yuneec MANTIS (see Figure 11). This micro UAV drone RCS polar plots are depicted in Figures 12 and results summarized in Table 4.

Fig. 11. Yuneec MANTIS drone

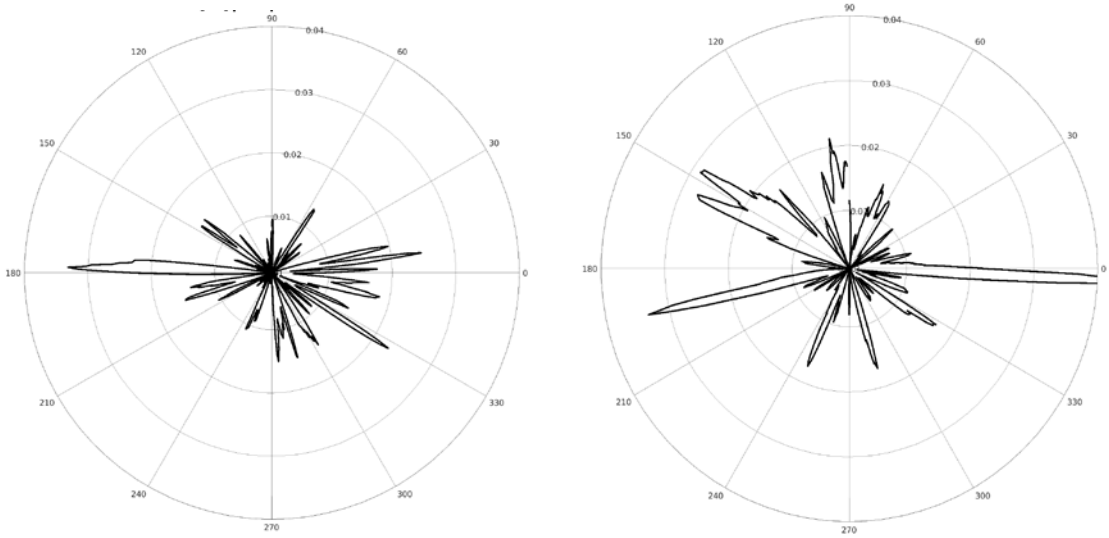

Fig. 12. Polar plot of MANTIS main plane RCS (left) and 5 degrees from top plane RCS (right); [sqm] @9 GHz.

Table 4. Yuneec Mantis RCS over azimuth statistics (@9 GHz)

Scenario	RCS [sqm]			
	max	median	mean	10th percentile
main	0.03	0.004	0.006	0
5 deg from the top	0.05	0.006	0.008	0.001
Pitch 29 deg	0.06	0.006	0.008	0.001
Roll 25	0.03	0.005	0.006	0.001

A representative of bigger (550 mm) drone was a hexacopter based on DJI DYI kit, see Figure 13. Polar plot of RCS is depicted in Figure 14. The RCS maximum was 0.29 sqm, median 0.03 sqm, mean 0.05 sqm and 10th percentile 0.004 sqm.

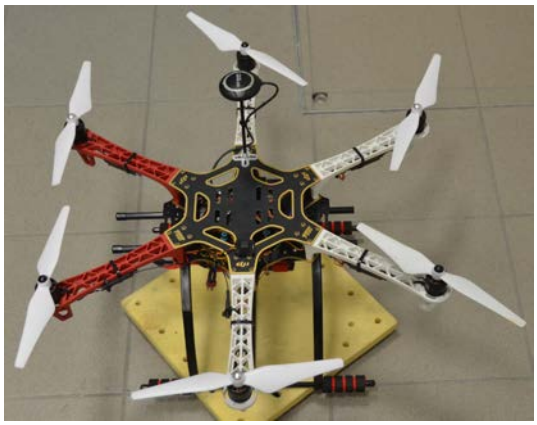

Fig. 13. DJI F550 drone.

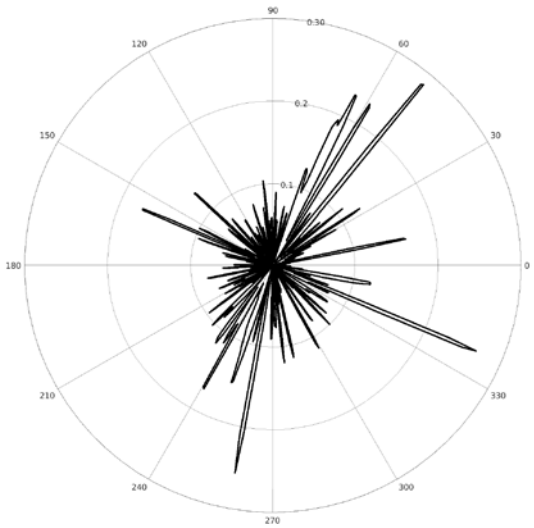

Fig. 14. Polar plot of F550 RCS [sqm] @9 GHz.

Coaxial copter drones are represented by Y6 (Figure 15) and X8 (Figure 17). Polar plots of RCS are depicted on Figure 16 and 18 respectively. The Y6 RCS maximum was 0.4 sqm, median 0.03 sqm, mean 0.05 sqm and 10th percentile 0.004 sqm. The X8 RCS maximum was 1.6 sqm, median 0.07 sqm, mean 0.12 sqm and 10th percentile 0.02 sqm. Significantly higher RCS of X8 drones is caused by high share of metallic components.

Fig. 15. A Y6 drone.

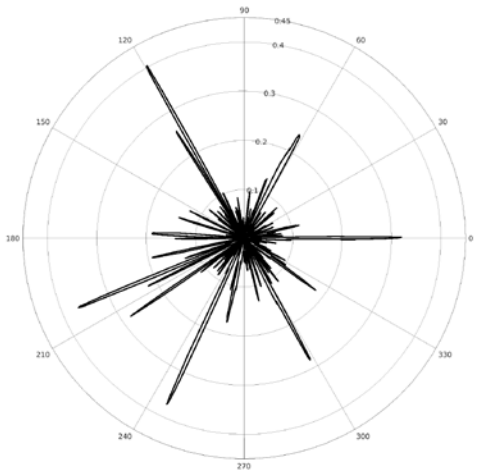

Fig. 16. Polar plot of Y6 RCS [sqm] @9 GHz.

Fig. 17. An X8 drone.

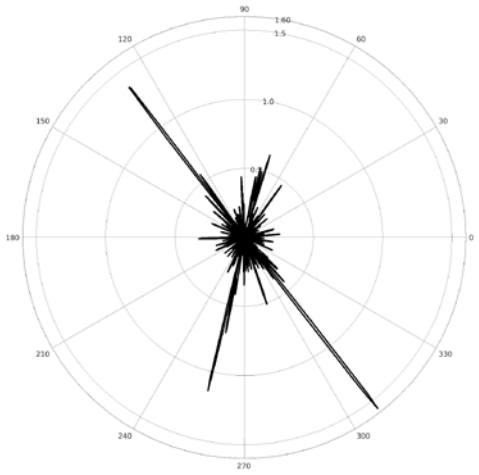

Fig. 18. Polar plot of X8 RCS [sqm] @9 GHz.

The biggest copter drones measured was Tarrot 680 (see Figure 19). Polar plots of RCS is depicted in figure 20. The RCS maximum was 0.85 sqm, median 0.06 sqm, mean 0.09 sqm and 10th percentile 0.008 sqm.

Fig. 19. An Tarrot 680 drone.

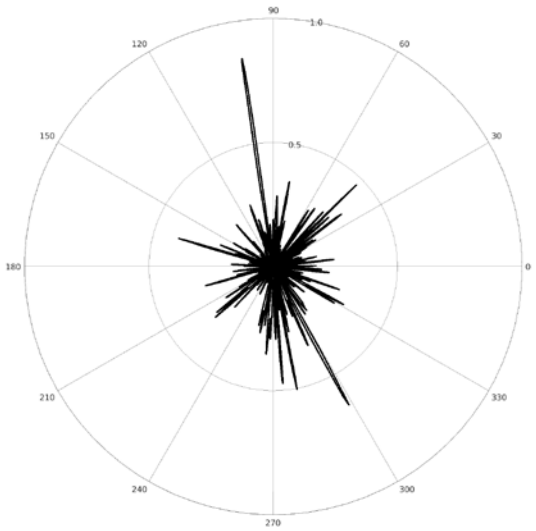

Fig. 20. Polar plot of Tarrot 680 RCS [sqm] @9 GHz.

A representative of fixed wing drone was Pelikan Gamma 2100 (see Figure 21). Polar plots of RCS is depicted in Figure 22. The RCS maximum was 0.1 sqm, median 0.01 sqm, mean 0.02 sqm and 10th percentile 0.002 sqm.

Fig. 21. A Gama 2100 drone.

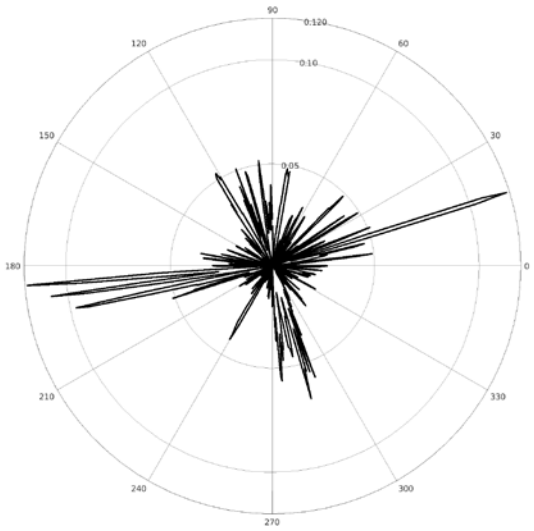

Fig. 22. Polar plot of Gama 2100 RCS [sqm] @9 GHz.

In addition to drone's RCS was measures RCS of a payload - an outdoor camera SJCAM SJ6 Legend (see Figure 23). Polar plots of RCS is depicted in Figure 24. The RCS maximum was 0.22 sqm, median 0.04 sqm, mean 0.05 sqm and 10th percentile 0.02 sqm.

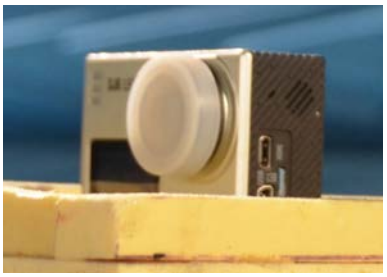

Fig. 23. A payload – SJ6 camera.

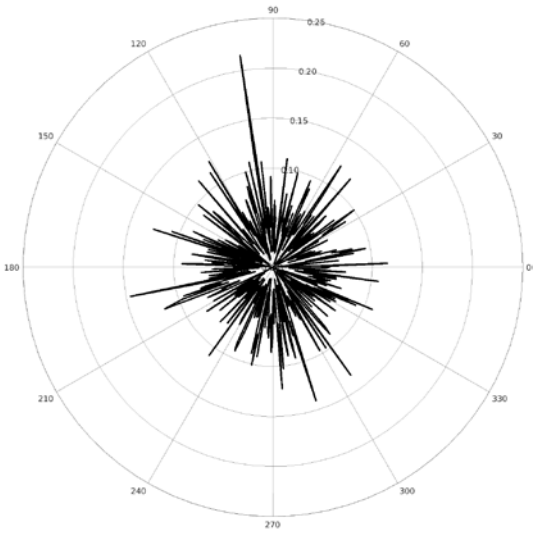

Fig. 24. Polar plot of SJ6 camera RCS [sqm] @9 GHz.

The RCS of Hornet drone 10” plastic propellers was not measured directly, only RCS of drone without propellers was measured. As the impact on drone RCS was negligible, propellers’ RCS is similar or smaller than anechoic chamber background RCS (bellow 0.001 sqm) and micro Doppler effect components for the smallest drones observed at low signal to noise ratios will be hidden in noise.

Another impact to RCS is frequency of radar signal. Radar echoes power (RCS) decorrelates once the radar signal carrier frequency differs by correlation frequency (1)[9].

$$f_c = \frac{c}{2L_r} \tag{1}$$

Where f_c is correlation frequency, c is the velocity of light and L_r is a distance of reflecting objects.

As the typical dimension of nano and micro UAVs is from 20 to 50 cm (considering motors reflection), correlation frequency should be about 500 MHz. The real frequency impact on DJI’s Phantom 4 RCS illustrates Figure 4. Frequency diversity observation introduces gain, but for real radar systems with relative bandwidth below 5%, no more than 2 independent samples can be obtained for X band.

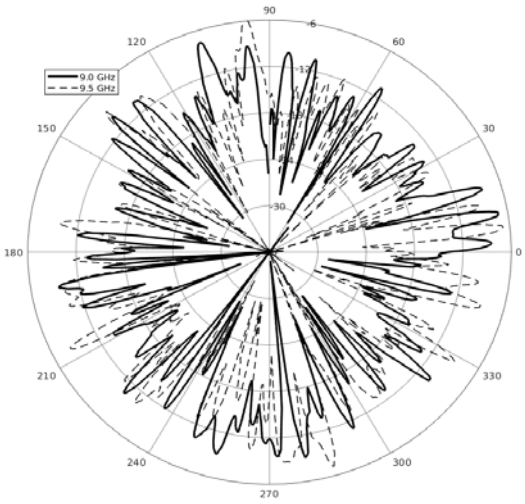

Fig. 25. Polar plot of Phantom 4 RCS [dBsm]

Impact of diversity frequency observation illustrates Figure 25. Bigger frequency change results more often in higher RCS diversity gain (difference of bigger and smaller observed RCS). Diversity gain cdf for selected set of measured drones is depicted on Figures 26 to 28. Diversity gain observed especially for higher deciles differs significantly for drones of different size. Another difference appears for observation frequency band/difference impact for individual drones.

Fluctuation losses and diversity gains for different drones are presented in Table 5. Values disclose negligible impact of fixed wings drone size (correlation frequency should be according to size lower(1)); this is probably caused by position of dominant reflector inside fuselage – much smaller distance of reflectors than wingspan.

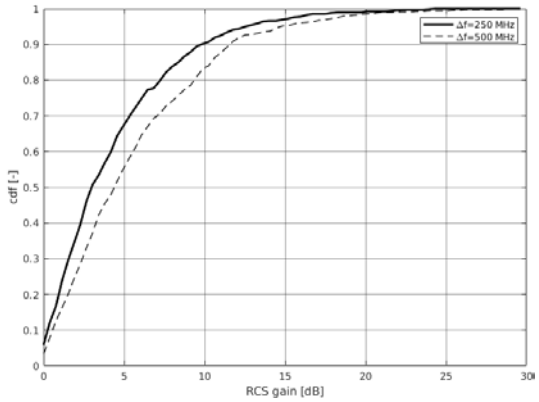

Fig. 26. Cumulative density function of Phantom 4 diversity gain

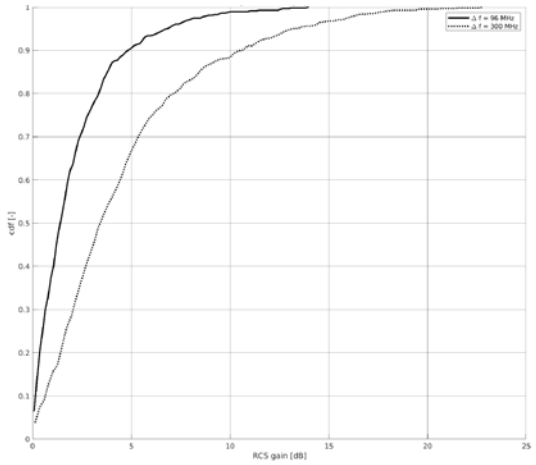

Fig. 27. Cumulative density function of MANTIS diversity gain

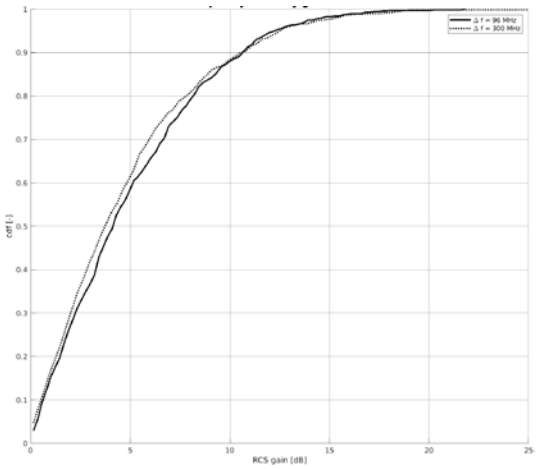

Fig. 28. Cumulative density function of fixed wing GAMA 2100 diversity gain

Table 5. Comparison of drones' fluctuation losses and diversity gain

Drone	Size [mm]	Fluct. losses P_{10}-median [dB]	Divers. Gain median, Δf=300 MHz [dB]
MANTIS	190	8.2	3.3
Phantom 4	350	8.6	3.3
F550	550	8.7	4
Tarrot	700	8.9	4
Gama2100	2100	6.8	3.5

4 FUTURE WORK

Presented research encourages many research activities in different areas, e.g. add data for more drones of different construction and configuration and evaluate the exact impact on primary radar detection performance. Another opportunity is utilized RCS frequency fluctuations for target classification –

distinguish groups of targets according to size. Another challenge is evaluation of RCS behaviour of birds – this can be done only by radar records analysis.

5 CONCLUSION

The drones' RCS is a phenomena too complex to be characterized by a single number. The RCS behaves much more like random variable. The paper analyses the drones' RCS measurement results and it's analysis.

Results of the RCS analysis can be used for the radar drone detection performance estimation improvement. Drones' RCS is presented as cumulative density function and statistics. Another outcome is estimate of drone's RCS gain caused by frequency diversity observation.

Another application opportunity of RCS behaviour analysis is contribution to target type classification. RCS changes with frequency should rely on target size.

REFERENCES

[1] Ch. Tsai, Ch. Chiang, W. Liao, Radar cross section measurement of unmanned aerial vehicles, IEEE Int. Workshop on Elmg.: App. and Student Innovation Competition (2016)

[2] A. Schroder, M. Renker, U. Aulenbacher, A. Murk, U. Böniger, R. Oechslin, P. Wellig, Numerical RCS and micro-Doppler investigations of a consumer UAV, IEEE Radar Conference (2015)

[3] Ch. J. Li, H. Ling, Radar Signatures of Small Consumer Drones, AP-S/USNC-URSI IEEE (2016), Purto Rico

[4] M. Ritchie, F. Fioranelli, H. Griffiths, B. Torvik, Micro-Drone RCS Analysis, IEEE Radar Conference (2015)

[5] E. Gopalakrishnan, Quadcopters Flight Mechanics Model And Control Algorithms, Master Thesis CTU Prague, (2017)

[6] SPK Drones, How Quadcopters Fly, https://www.spkdrones.com/how-quadcopters-fly/

[7] ArduPilot Dev Team, Ardupilot, https://firmware.ardupilot.org/Copter/

[8] Á. D. de Quevedo, F. I. Urzaiz, J. G. Menoyo, A. A. López, Drone Detection and RCS Measurements with Ubiquitous Radar, International Conference on Radar (2018) Brisbane

[9] D. K. Barton, Radar Equations for Modern Radar, Artech House, ISBN: 978-1608075218, (2012)